PGC PUBLISHING

Knight, J., Joy, S., Cameron, J., Merrillees, J., Nag, S., Shah, N., Dua, G. & Jhala, K., 2002 - The Khetri Copper Belt, Rajasthan; Iron Oxide Copper-Gold Terrane in the Proterozoic of NW India; *in Porter, T.M. (Ed.), Hydrothermal Iron Oxide Copper-Gold & Related Deposits: A Global Perspective,* Volume 2; PGC Publishing, Adelaide, pp 321-341.

THE KHETRI COPPER BELT, RAJASTHAN: IRON OXIDE COPPER-GOLD TERRANE IN THE PROTEROZOIC OF NW INDIA

[1]Joe Knight, [2]Sojen Joy, [1]Jon Lowe, [2]John Cameron, [2]James Merrillees, [2]Sudipta Nag, [2]Nalin Shah, [2]Gaurav Dua & [2]Khamalendra Jhala

[1]*BHP Billiton Exploration, Brisbane, Australia*
[2]*BHP Billiton Minerals India, New Delhi, India*

Abstract - The Khetri, Alwar and Lalsot-Khankhera Copper Belts contain widespread Cu±Au±Ag±Co±Fe±REE±U mineralisation over a 150x150 km area of Rajasthan and Haryana, NW India. Mineralisation is hosted by the mid-Proterozoic Delhi Supergroup, which comprises shallow-water, locally evaporitic, sedimentary rocks, with lesser mafic and felsic volcanic rocks. These rocks have been metamorphosed to the low- to mid-amphibolite facies, deformed into NE-SW striking, doubly-plunging folds, and intruded by numerous 1.5-1.7 Ga syntectonic granitoids and 0.75-0.85 Ga post-tectonic granitoids. Post-tectonic granitoids range from tonalite to syenite, contain hornblende and biotite as the dominant mafic minerals and magnetite, titanite, allanite, apatite, fluorite as accessory phases, and are geochemically characterised by A/CNK ratios <1.1, low Al and Ca, high Th and HFSE, and enrichment in LREE, indicating A-type affinities.

The largest deposits in the Khetri Copper Belt are at Khetri (140 mt @ 1.1-1.7% Cu, 0.5 g/t Au), where mineralisation extends over a >10 km strike-length, is hosted by garnet-chlorite schists, andalusite- and graphite-bearing biotite schists, and feldspathic quartzites, and is sited in sub-vertical NE- and NW-striking shear zones. Mineralisation forms sub-vertical lens, comprising stockworks of massive to vein-hosted chalcopyrite-pyrite-pyrrhotite, which are broadly foliation-parallel but also cross-cut bedding and peak-metamorphic fabrics. Gold, Ag, Co, LREE, Mo, S, U and W are variably co-enriched with Cu. Alteration at Khetri comprises amphibole (hornblende, actinolite, cummingtonite, anthophyllite)-albite-quartz-biotite-scapolite-chlorite-carbonate, with magnetite and haematite as dominant oxide phases.

Directly to the east of Khetri, a 50 km wide by > 100 km zone of calc silicate and albite-haematite alteration overprints and cross-cuts metamorphic fabrics. Calc silicate alteration comprises coarse-grained clinopyroxene-hornblende-epidote-apatite-scapolite-titanite-magnetite, whereas albite-haematite alteration comprises assemblages of albite-amphibole-haematite-magnetite-calcite, with variable K-feldspar, biotite, epidote, scapolite, titanite, apatite and fluorite, and locally abundant pyrite and chalcopyrite. Albite-haematite alteration is spatially related to vein systems and breccias, which commonly contain Cu-Au mineralisation, massive magnetite-haematite vein-deposits, fluorite mineralisation and rare uraninite deposits. Calc silicate alteration occurs on the margins of the Khetri Copper Belt, whereas albite-haematite alteration forms a central core to the Belt and locally overprints calc-silicate assemblages. A SHRIMP U-Pb titanite age in the assemblage albite-haematite-amphibole-calcite-titanite constrains the timing of regional alteration to 847±8 Ma. This overlaps the fission-track ages of garnet from ore assemblages at the Madhan-Kudhan Cu mine at Khetri (897±125 Ma).

There is a variation in the sulphide-oxide mineralogy of Cu deposits across the >100 km wide Khetri Copper Belt, with four dominant types recognised: (1) chalcopyrite-pyrite-pyrrhotite ores hosted by graphitic schists at Akwali, in the west, (2) chalcopyrite-pyrite-pyrrhotite-magnetite-haematite ores at Khetri and Kho Dariba, in the east, (3) magnetite-haematite-chalcopyrite-pyrite ores hosted by albite-haematite alteration, in the central part of the Khetri Copper Belt, and (4) haematite-chalcopyrite-baryte ores in the eastern part of the Belt. Types (1) and (2) are hosted by mainly reduced rock types and can be classified as iron sulphide Cu-Au deposits, whereas types (3) and (4) are iron oxide Cu-Au deposits hosted by oxidised rocks. Copper mineralisation in the Khetri Copper Belt is epigenetic, broadly synchronous with late (0.75-0.85 Ga) A-type granitoid emplacement, and has a mineralisation and structural style, and regional- and deposit-scale alteration assemblages comparable to known IOCG and iron-sulphide Cu-Au mineralised districts.

Introduction

Recent research on iron oxide copper-gold (IOCG) deposits has highlighted the diverse styles of mineralisation within this important deposit class (eg., Haynes, 2000; Hitzman, 2000). Hitzman et al. (1992) and Hitzman (2000) document a continuum of IOCG deposit-styles, from magnetite-apatite deposits to iron oxide copper-gold deposits. Haynes (2000) describes a broader transition from iron-oxide Cu-Au deposits, in which Cu sulphides are associated with dominant magnetite or haematite, to iron sulphide Cu±Au deposits, in which chalcopyrite is associated with abundant pyrrhotite and pyrite. The mineralogy and metal-associations of these deposits are controlled by the depth and temperature of mineralisation, the composition of the mineralising fluid (s), and the oxidation states of host-rocks to ore (Haynes, 2000). Iron oxide Cu-Au deposits are hosted by oxidised rocks, whereas iron-sulphide Cu-Au deposits are mainly hosted by reduced carbon-bearing rocks. Unifying features of IOCG and iron sulphide Cu±Au deposits in a given terrane are the association of Cu-mineralisation with regional-scale fault-controlled sodic alteration, comprising albite, magnetite, haematite, actinolite, with variable scapolite, chlorite, epidote, carbonate and titanite, the dominantly brittle nature and late-timing of ore-hosting structures, a likely common hydrothermal-fluid source and composition, and a similar timing of ore deposition (Haynes, 2000).

In this paper, a range of IOCG and iron sulphide Cu-Au deposits are described from the Khetri, Alwar and Lalsot-Khankhera Copper Belts located in Rajasthan and Haryana States, NW India. These Belts form a 150x150 km NE-striking zone of rocks, which hosts numerous Cu±Au±Ag±Ba±Co±Fe±Mo±U±REE deposits (Fig. 1). Host rocks to mineralisation are metamorphosed

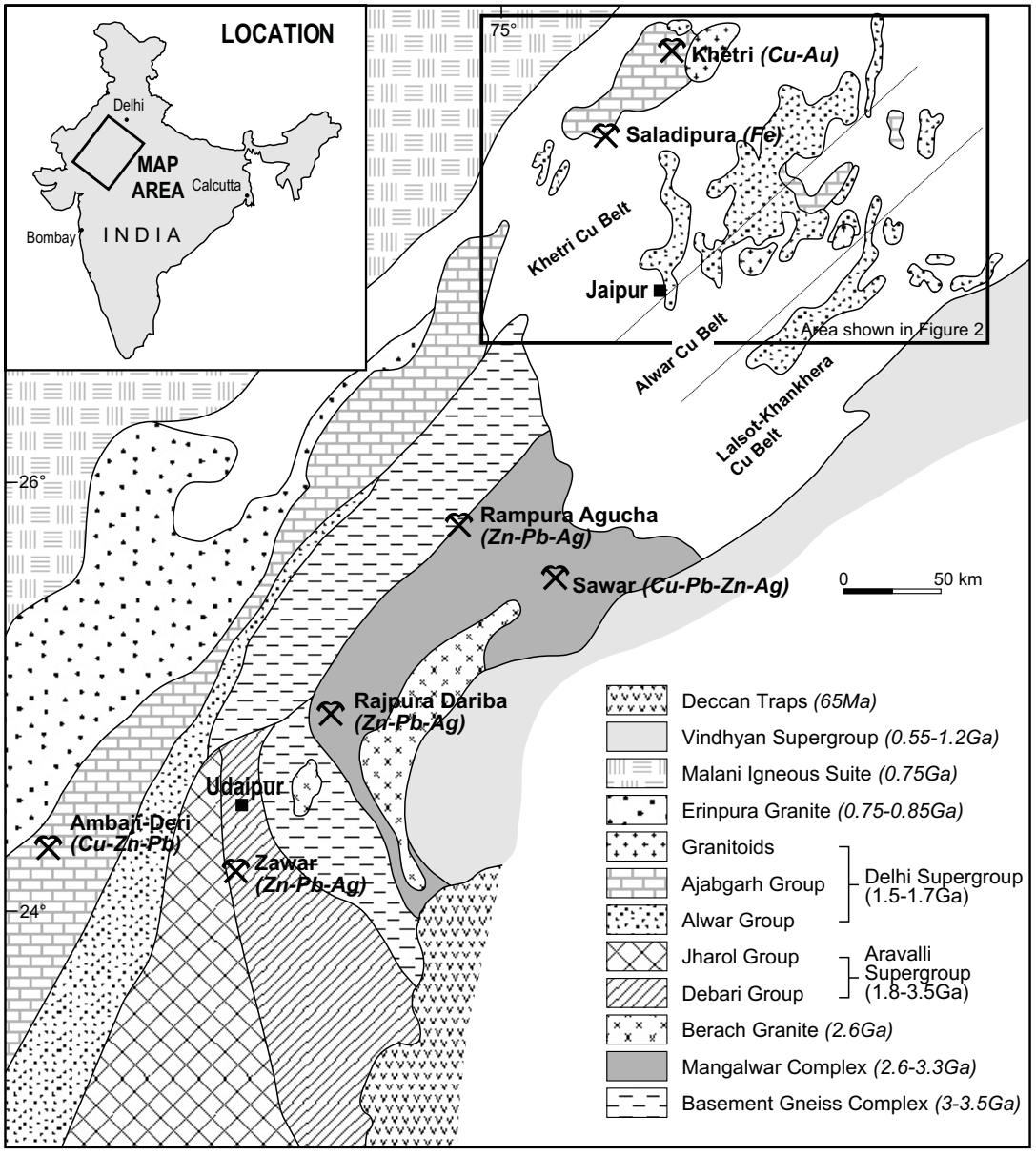

Figure 1. Simplified geology of Southern Rajasthan showing locations of major base metal deposits.

volcano-sedimentary rocks of the mid-Proterozoic Delhi Supergroup and, as demonstrated below, Cu deposits within these Belts display common structural controls, ore and alteration mineralogy, and geochemical associations. All belts are therefore described here and the entire copper-mineralised region is referred to as the Khetri Copper Belt (KCB). The KCB is located in the north of Rajasthan which contains major mid-Proterozoic Pb-Zn-Ag deposits at Rampura Agucha (61 Mt @ 13.47% Zn, 1.93% Pb, 45 g/t Ag), Rajpura Dariba (20 Mt @ 2% Pb, 7% Zn, 100 g/t Ag) and Zawar (45 Mt @ 2% Pb, 4% Zn, 50 g/t Ag), and massive pyrite-pyrrhotite±base-metal sulphides deposits at Saladipura (Fig. 1).

Three main models have been proposed for the genesis and timing of mineralisation in the KCB: (1) syngenetic models where the ores formed during sedimentation or diagenesis and were subsequently metamorphosed (eg., Sarkar et al., 1974; Sarkar and Dasgupta, 1980; Basu 1986), (2) hydrothermal models in which mineralisation formed epigenetically, synchronous with, and potentially genetically related to, late granitoid-emplacement (Roy Chowdhury and Das Gupta, 1965; Banerjee 1976) and (3) a combination of models (1) and (2) involving syngenetic mineralisation with subsequent remobilisation and overprinting hydrothermal mineralisation (eg., Das Gupta, 1974). Other research has alluded to the presence of iron oxide copper gold (IOCG)-associated regional alteration in the KCB. Heron (1922), Ray (1987) and Ray and Ghosh (1989) documented the occurrence of 'albitites' in the Khetri region. Ray (1990) defined the "Albitite Line" of northern Rajasthan, a 170 km NNE-trending lineament extending SW from Khetri, characterised by intrusions of albitite, comprising massive pink-red equigranular albite. Das Gupta (1968), Basu and Narsayya (1982, 1983) and Ray (1987, 1990) documented widespread albitisation, fenitisation and Fe-Ti oxide-uraninite-molybdenite-Cu-Fe sulphide-fluorite-calcite mineralisation in the northern part of the KCB and interpreted an igneous origin for the "albitites". Ray (1990) proposed that the "Albitite Line" represents a major intracontinental rift system. In none of these papers however, were the alteration characteristics linked to the Cu deposits at Khetri or the widespread Cu mineralisation in the KCB.

This paper describes the regional geological setting, and nature of wallrock alteration and mineralisation in the KCB, and proposes that Cu±Au±Ag±Co±Fe±REE±U mineralisation was deposited after regional deformation and metamorphism. Furthermore, it is demonstrated that the KCB hosts a range of iron oxide Cu-Au and iron sulphide Cu-Au deposits within a regional-scale calc silicate and sodic alteration system.

Regional Geology

Stratigraphy

The KCB is hosted by the >5 km thick Delhi Supergroup (eg., Singh, 1988), which comprises the basal Raialo Group (metamorphosed carbonate, conglomerate and sandstone, mafic and felsic volcanic rocks), overlain by the Alwar Group (metamorphosed conglomerate and sandstone), which is overlain in turn by the Ajabgarh Group (metamorphosed stromatolitic carbonate, siltstone and shale). Minor felsic and mafic volcanic rocks occur throughout the Ajabgarh and Alwar Groups. Within the KCB, a regionally-continuous, stratigraphically-conformable breccia horizon crops-out. This horizon, named the Hornstone Breccia (Heron, 1917), is broadly at the contact between the Alwar and Ajabgarh Groups (Gangopadhyay, 1974) and comprises angular fragments of quartz and quartzite in a massive Fe-rich chert matrix. It may represent a breccia formed by evaporite dissolution (cf., Corella Formation, Mt Isa: Blake et al., 1990). Outcrop in the KCB is dominated by Alwar Group quartzites, which vary from fine-grained equigranular pure quartzite, to weakly feldspathic quartzite and sericitic quartzite. Towards Jaipur and around Kalyanpura, coarse-grained poly-mictic conglomerates are developed. These rocks comprise matrix-supported conglomerates, with subrounded clasts of quartz, chert, carbonate and meta-siltstone. Banded, locally brecciated, amphibole-bearing dolomitic marble also crops out.

The Delhi Supergroup was likely to have been deposited within a series of intra-cratonic rift basins, developed on Archaean basement rocks, with the depositional environment varying from shelf/shallow marine to fluvial (Singh, 1988; Deb and Sarkar, 1990). Dasgupta (1978) suggested a lagoonal, evaporitic environment for the Ajabgarh Group. The depositional age of the Delhi Supergroup rocks is not known; however, the minimum age is constrained to 1691±4 Ma, the SHRIMP U-Pb in zircon age of the syn-tectonic Gothra Granite, east of Khetri (data from this study, see below). Other estimates of the depositional age of the Delhi Supergroup are based on the 1.5-1.7 Ga Rb-Sr whole-rock ages of syn- and pre-tectonic granitoids (Crawford, 1970; Choudhary et al., 1984).

Metamorphism and Structure

Rocks of the Delhi Supergroup have been metamorphosed to the low- to mid-amphibolite facies. Typical metamorphic mineral assemblages are hornblende-plagioclase-garnet in unaltered mafic rocks, and biotite-muscovite-andalusite-sillimanite, staurolite-garnet-muscovite-biotite-quartz and biotite-chlorite-garnet-amphibole in pelitic rocks (Gangopadhyay and Sen, 1967). Lal and Shukla (1975) estimated peak metamorphic conditions to be 500-600°C at 3-5 kb in the northern part of the KCB using mineral equilibria. Sarkar and Dasgupta (1980) estimated similar metamorphic conditions at Khetri (550-600°C at <5.5 kb).

Two main phases of deformation can be recognised in the KCB: early ductile-deformation and late brittle-deformation. Primary rock types contain a sub-vertical, NE-striking foliation, defined by peak metamorphic minerals, and a steeply plunging mineral lineation. The foliation is axial-planar to NNE-trending regional-scale, locally over-turned, doubly-plunging folds, which have been refolded by a set of NW-trending cross folds. These early structures are cross-cut by NE- and NW-striking brittle and brittle-ductile faults, which play an important

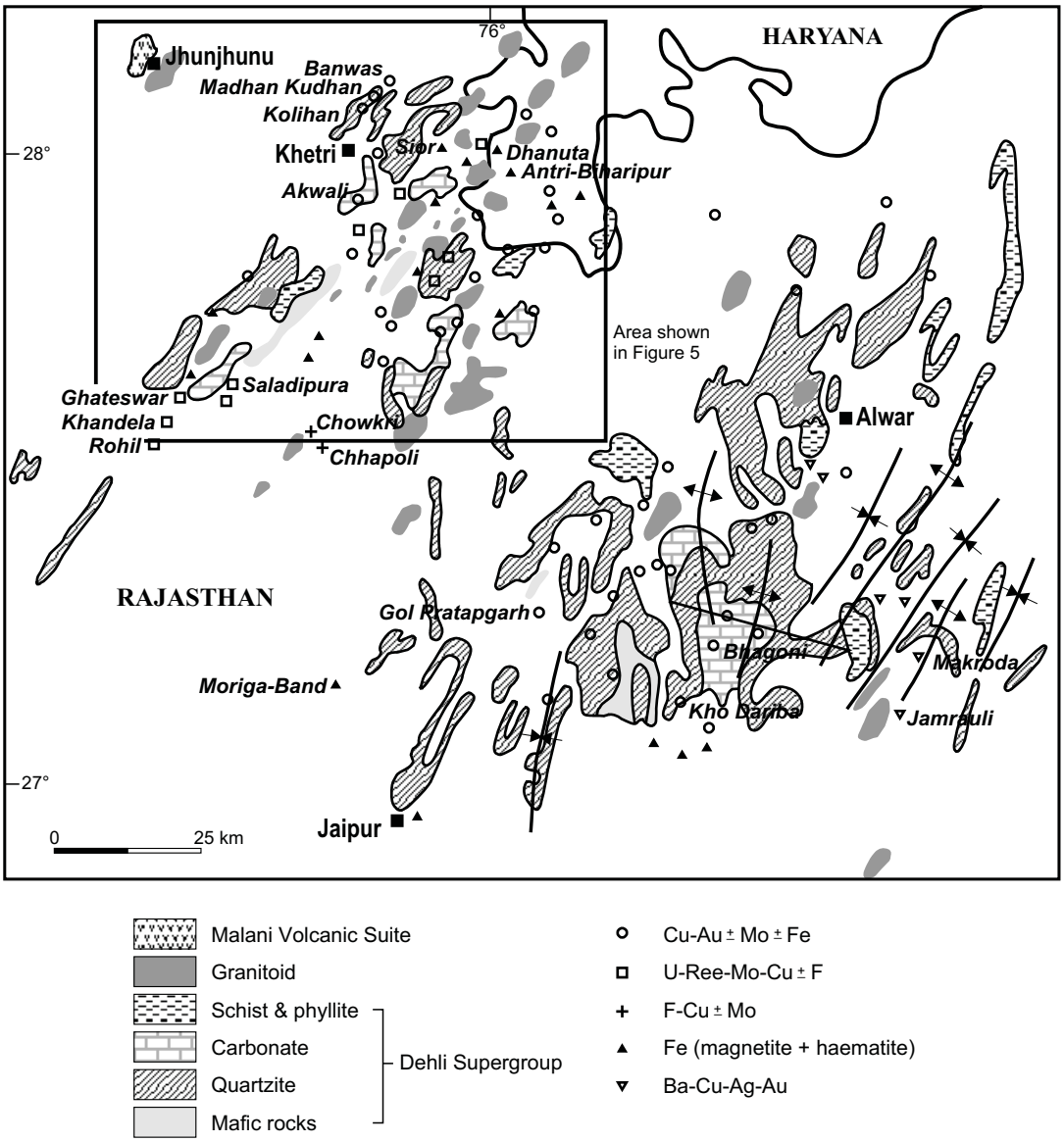

Figure 2. Simplified outcrop geology of the Khetri Copper Belt, Rajasthan showing locations of mineral deposits.

role in controlling mineralisation and alteration, and are overprinted by late brittle structures (stockworks, breccias, quartz veins), associated with regional alteration (see below).

Granitoids

The KCB is intruded by several poorly exposed granitoids (Fig. 2), which vary from foliated completely-recrystallised bodies, intruded along the axes of regional NNE-trending folds (eg., the Gothra Granite), to small-diameter (<5-10 km) undeformed ovoid stocks that overprint, and therefore probably post-date, peak deformation fabrics. Granitoids range in composition from composite bodies of grey-white tonalite and pink-red syenite, to homogeneous massive pink-red syenite (eg., Bairat), and porphyritic grey tonalite (eg., Sainthal and Pragpura Granites). Foliated granitoid at Ramgarh comprises porphyritic granite-tonalitic granite with minor secondary muscovite.

The pre- or syntectonic, foliated Gothra Granite, located to the east of the Cu-Au deposits at Khetri, is characterised by strong enrichment in the LREE, depletion in the HREE (Fig 3a), no Eu anomaly and a strongly fractionated REE pattern (La_n/Yb_n = 240). The granitoid is enriched in Th and HFSE, and has a very high Na_2O content (8.30%). Primary calcic plagioclase and K-feldspar within the Gothra Granite have been widely replaced by secondary albite, and pods and veins of amphibole-epidote-haematite-feldspar cross-cut the granitoid. In combination, these characteristics suggest that the Gothra Granite has been hydrothermally altered.

Post-tectonic granitoids in the KCB have hornblende and biotite as the dominant mafic minerals and contain magnetite, titanite, allanite, apatite, fluorite and tourmaline as common accessory phases. These granitoids are alkali-rich and meta-aluminous (A/CNK<1.1), with Na/K ratios varying from <1 to >20 (Table 1). Silica contents

Table 1: **Geochemistry of granitoids from the Alwar and Khetri regions, Rajasthan**

	Gothra	Saladipura	Jat Ki Dhani	Ajit Garh	Ajit Garh	Bairat	Sainthal	Pragpura	Ramgarh
Major elements									
SiO_2 (%)	70.80	69.52	76.58	77.43	76.15	76.58	73.80	73.80	72.51
TiO_2 (%)	0.28	0.58	0.50	0.45	0.45	0.07	0.28	0.27	0.50
Al_2O_3 (%)	13.51	13.09	10.58	11.94	12.07	12.01	14.19	13.15	11.75
Fe_2O_3 (%)	2.67	4.79	3.52	2.16	5.48	1.02	2.99	2.86	4.16
MnO (%)	0.03	0.04	0.02	0.01	0.03	0.01	0.03	0.04	0.03
MgO (%)	0.35	0.76	0.46	0.40	0.32	0.25	0.41	0.48	0.93
CaO (%)	0.71	1.76	0.95	1.44	1.90	0.27	0.84	1.13	0.91
Na_2O (%)	8.30	2.74	4.57	7.43	3.88	7.49	3.22	2.59	2.25
K_2O(%)	0.52	5.64	3.18	0.31	4.78	0.34	7.37	6.10	5.96
P_2O_5 (%)	0.26	0.17	0.08	0.09	0.07	0.01	0.24	0.26	0.41
A/CNK	1.01	0.87	0.83	0.93	0.78	1.05	0.82	0.89	0.86
Na/K	14.33	0.43	1.28	21.19	0.73	19.86	0.39	0.38	0.34
Trace elements									
Ba	117	1080	191	55	1110	213	837	405	763
Hf	6.4	3	5.8	5	5.8	5.2	3.4	2.6	4.4
Li	2.5	25	3	6.5	22.5	15	51	35	81.5
Nb	10.5	21	29.5	27	28	18.5	21.5	18.5	35.5
Rb	20.3	245	98.8	7.2	149	30	496	352	492
Sr	29.6	106	10.7	12.8	38.6	11.1	94.4	61	60.2
Ta	1.1	1.7	3.15	1.9	2.5	2.6	2.25	1.5	3.95
V	40	34	24	20	14	8	16	18	34
Y	32.7	59.8	80.5	82.4	91.6	36.3	30.4	15.9	41
Zr	219	110	199	160	175	116	114	94	155
U	8.8	2.35	6.35	3.85	6.2	17.5	16.3	4.65	10.9
Th	85.3	37.3	41	28.5	28.8	74	34.5	28.3	43.5
Metals and ore elements									
Au (ppb)	bdl	bdl	bdl	bdl	bdl	bdl	1	bdl	bdl
Ag	bdl	bdl	bdl	bdl	bdl	bdl	bdl	bdl	bdl
Bi	bdl	bdl	bdl	0.1	0.8	bdl	0.3	0.1	2.3
Cu	67	10	15	10	15	44	101	119	62
Mo	3	1.2	0.4	2.6	2.2	1.8	2	0.4	2.4
Ni	8	8	4	4	6	6	42	8	10
Pb	10	26	3	8	40	8	53	45	27
Pt (ppb)	bdl	bdl	bdl	bdl	bdl	bdl	bdl	bdl	bdl
Pd (ppb)	bdl	bdl	bdl	bdl	bdl	bdl	bdl	bdl	bdl
S	100	60	40	40	140	60	120	220	120
Sb	bdl	bdl	bdl	bdl	bdl	bdl	bdl	bdl	bdl
W	1	1	bdl	0.5	1	1	1.5	1.5	3.5
Zn	13	47	11	22	23	11	66	55	36
Rare earth elements									
La	870	86.1	79.9	33.5	74.1	38.4	46.3	37.9	66.1
Ce	1680	196	130	104	151	65.4	101	84.9	146
Pr	167	20	18	14.6	17.1	8.02	11.3	10.1	17.1
Nd	523	71.6	71	62.5	66.1	27.6	42	37.3	63.5
Sm	81.6	13	14.6	14	14.5	5.6	8.6	8.05	11.7
Eu	15.5	1.64	1.82	2.16	2.32	0.4	0.88	0.58	0.72
Gd	51.6	11.2	14.6	14.4	14.6	5.2	7.2	6.8	9.2
Tb	4.48	1.72	2.36	2.28	2.36	0.94	1	0.9	1.3
Dy	14.2	10.7	15.5	14.9	15.3	6	6.1	4.2	7.45
Ho	1.54	2.12	3.08	3.06	3.2	1.34	1	0.56	1.38
Er	3.65	6.3	9.3	8.9	9.6	4.45	2.75	1.1	3.75
Tm	0.38	0.92	1.38	1.3	1.4	0.76	0.38	0.12	0.54
Yb	2.4	5.85	9.45	8.25	9.2	5.25	2.25	0.6	3.3
Lu	0.3	0.8	1.4	1.16	1.34	0.78	0.3	0.06	0.42
(La/Lu)n	294.6	10.9	5.8	2.9	5.6	5.0	15.7	64.2	16.0
(La/Yb)n	239.4	9.7	5.6	2.7	5.3	4.8	13.6	41.7	13.2
Eu*	0.7	0.4	0.4	0.5	0.5	0.2	0.3	0.2	0.2
La/Sm	6.5	4.0	3.3	1.5	3.1	4.2	3.3	2.9	3.4
Gd/Yb	17.3	1.5	1.2	1.4	1.3	0.8	2.6	9.1	2.2
Total REE	3415.7	428.0	372.4	285.0	382.1	170.1	231.1	193.2	332.5

Elements were analysed using a combination of ICP-MS and ICP-OES techniques. Bdl = below detection limit.

are generally uniform (69.5-77.4%), and the granitoids have low Al and Ca, high Th (28.3-85.3 ppm) and moderate enrichment in the HFSE (Fig 3b). Post-tectonic granitoids in the Khetri region are moderately enriched in LREE, moderately depleted in HREE, have pronounced negative Eu anomalies (Fig. 3a), and weakly fractionated REE patterns (La_n/Yb_n varies from 2.7 to 41.7). These mineralogical and geochemical features indicate that post-tectonic granitoids in the KCB have affinities with A-type granitoids (cf., Whalen et al., 1987).

Available age determinations indicate two main phases of granitoid emplacement within the KCB. Pre- and syn-tectonic granitoids have whole-rock Rb-Sr ages from 1.5-1.7 Ga (Crawford, 1970; Choudhary et al., 1984). Gopalan et al. (1979) calculated a whole-rock Rb-Sr age of 1480±40 Ma for the Udaipur and Saladipura granitoids in the southern KCB. The altered Gothra Granite, to the east of Khetri, has a SHRIMP U-Pb in zircon age of 1691±4 Ma (Fig. 4a and Appendix 1). Zircon U-Pb and Rb-Sr whole rock ages of 0.75 to 0.85 Ga characterise post-tectonic granitoids throughout southern Rajasthan, including the KCB (Crawford, 1970; Deb et al., 2001). This suite probably forms part of the so-called Erinpura Suite of granitoids, which comprises a suite of post-tectonic batholiths, comprising pink-white porphyritic granitoids, located to the SW of the KCB (Heron, 1953, Fig. 1).

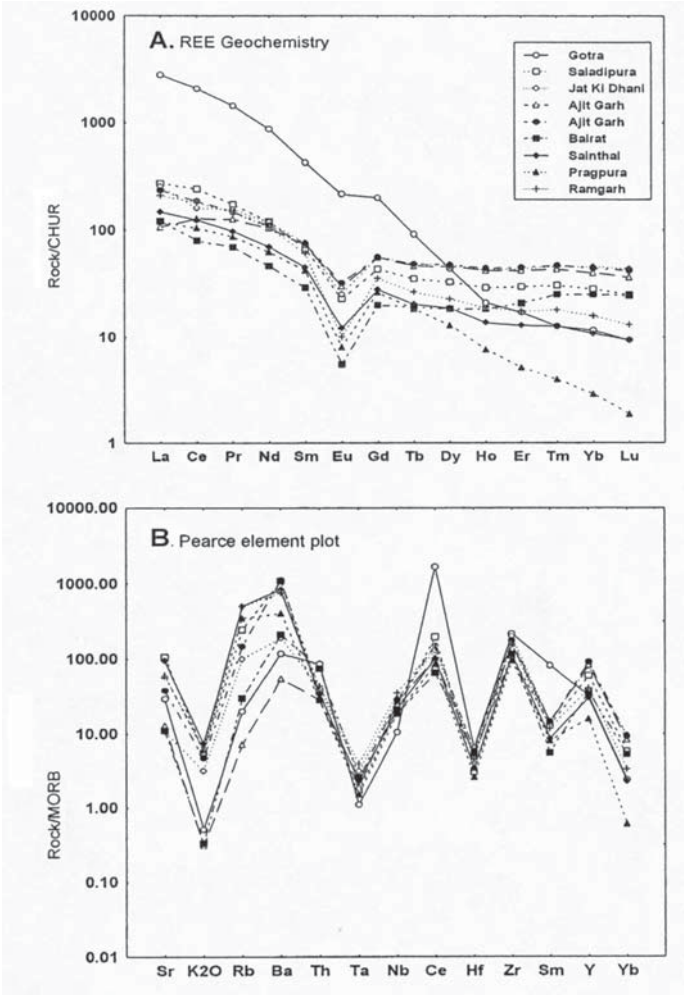

Figure 3: Geochemistry of granitoids in the KCB.
A. Chondrite-normalised REE plot (normalisation factors from Nakamura, 1974).
B. MORB normalised spider plot (element order after Pearce,

Nature of Mineralisation in the KCB

The largest Cu deposits in the KCB occur at Khetri, which has a total resource of around 140 million t @ 1.1-1.7% Cu and 0.5 g/t Au (production and resources: unpublished Hindustan Copper Ltd data). Smaller Cu deposits occur at Akwali, SW of Khetri, and at Kho Dariba (<1 million t @ 2.5 % Cu) and Bhagoni (5.2 million t @ 1.07% Cu) in the eastern part of the KCB. These deposits are described in further detail below. Numerous other Cu, Cu-Au and Cu±Au±Ag±Co±U±REE prospects have been identified, and partly explored, by the Geological Survey of India throughout northern Rajasthan and the southern part of Haryana (Fig. 2).

Nature of Cu Mineralisation at Khetri

Copper mineralisation at Khetri occurs over a >10 km curvilinear NE-strike length (Fig. 5), which broadly parallels the transition from quartzite-carbonate dominant sequences to the east, to biotite- and andalusite bearing schists to the west. Economic concentrations of Cu and Au at Khetri occur at Madhan Kudhan (66 million t @ 1.12-1.71% Cu, 0.2-0.6 g/t Au, 2-8 g/t Ag), Kolihan-Chandmari (production and resources of around 40 million t @ 1.14-1.62% Cu, 0.2 g/t Au, 2 g/t Ag) and Banwas (resources of around 30 million t @ 1.7% Cu, 0.5-1 g/t Au).

Banwas/Madhan-Kudhan

Mineralisation at Madhan-Kudhan and Banwas is hosted by steeply west-dipping andalusite-bearing phyllites, amphibole-bearing quartzites and garnet-chlorite-amphibole schists, and forms a series of discontinuous layer sub-parallel lodes (Fig. 6a and b). Within lodes, sulphide mineralisation forms: (1) massive zones of pyrite-chalcopyrite-calcite, (2) quartz-chalcopyrite-pyrite-pyrrhotite vein sets (Fig 7a), (3) pyrrhotite-chalcopyrite-amphibole-calcite lenses, and (4) chalcopyrite-pyrrhotite stringers and veinlets. Chalcopyrite-pyrrhotite mineralisation is also hosted by garnet-chlorite-amphibole rock at Madhan Kudhan (Fig. 7b).

Kolihan-Chandmari

In Chandmari, mineralisation is hosted by quartzites, which show a gradation in amphibole and feldspar content across the deposit, with Cu-Au mineralisation broadly sited along the transition between hornblende-bearing and albite-bearing quartzites (Fig. 6d). Mineralisation forms (1) massive amphibole-chalcopyrite-pyrrhotite rock, characterised by a transition in amphibole composition from pale tremolitic amphibole in altered wallrocks to dark green hornblende in ore, (2) massive undeformed quartz-chalcopyrite-pyrrhotite veins, enveloped by albite-hornblende alteration, which cross-cut the regional amphibolite-facies fabric (Fig. 7c), (3) quartz-calcite-chalcopyrite veins, with biotite-chlorite alteration, and (4) stockworks of amphibole-biotite-chalcopyrite-pyrrhotite-magnetite veins (Fig. 7d). Type 1 mineralisation forms the main ore horizon, with types 2, 3

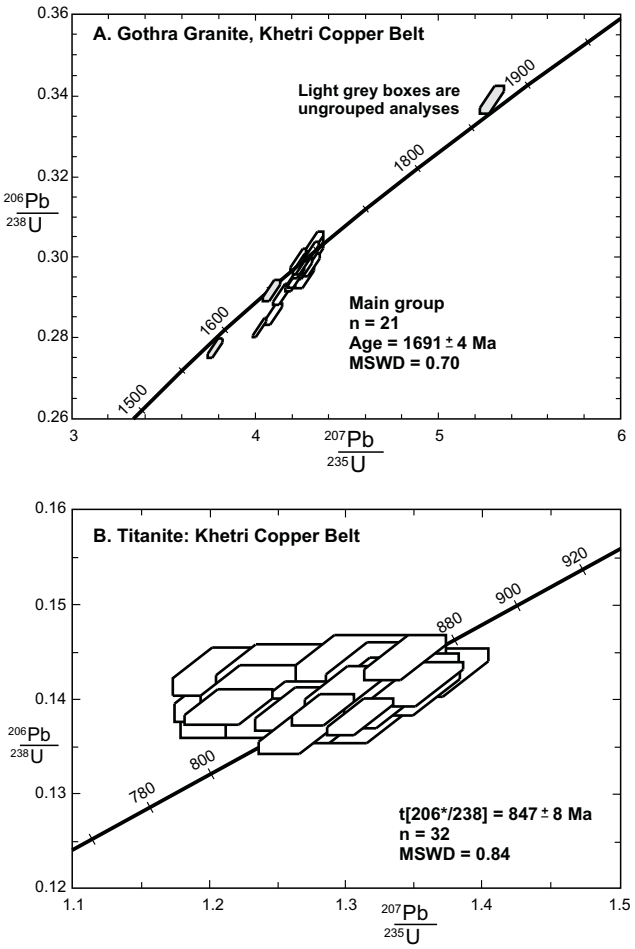

Figure 4: Shrimp II analyses from:

- **A.** Zircons from the Gothra Granite
- **B.** Titanite from regional alteration. Error boxes are 1σ analytical data are tabulated in Appendix 1.

and 4 hosted in hanging-wall and footwall alteration zones. Disseminated carbonate and magnetite are associated with all styles of mineralisation. Mineralisation at Kolihan is hosted by garnet-chlorite-amphibole schist and comprises massive amphibole-chlorite-chalcopyrite-pyrrhotite-garnet rock with quartz-chalcopyrite-pyrrhotite veins in adjacent wallrocks.

Structural Controls

Mineralisation at Khetri is sited along NE- and NW-striking faults, which cross-cut and therefore post-date regional peak-metamorphic fabrics. At the deposit-scale, orebodies are broadly located along NE-striking faults which are preferentially developed along lithological contacts which dip 40-65° to the W. Sulphide-rich ore-shoots are located at the intersection of steeply-dipping faults. Mineralisation at Madhan Kudhan forms a subvertical cylinder-shaped body at the intersection of NE- and NW-striking faults (Roy Chowdhury and Das Gupta, 1965, Fig. 6a). Other ore bodies at Khetri form series of *en echelon* lenticular lodes, comprising vein sets, breccias and stockworks, which sub-parallel fault zones (Fig. 6). At the vein-scale, mineralised veins and stockworks cross-cut layering and peak metamorphic fabrics. Quartz in mineralised veins at Khetri forms clear, unstrained euhedra and there is little fabric development or evidence of deformation of ore.

Khetri Alteration Assemblages

At the lode-scale, wallrock alteration assemblages contain amphibole, albite, biotite, chlorite and calcite with variable amounts of scapolite, sericite, quartz, magnetite and haematite, and are developed for up to 30-50 m into adjacent wallrocks. Minor magnetite and haematite are disseminated through mineralised veins and altered wallrocks. Distal to mineralisation (>30-50 m), quartzite host rocks contain 10-15% disseminated amphibole, forming radial growths which cross-cut peak metamorphic fabrics. Massive, locally-brecciated Fe carbonate-albite-amphibole-magnetite-epidote±chalcopyrite rocks are developed for several hundreds of metres into the footwall of Cu lodes at Khetri.

These rocks grade into quartzites, feldspathic quartzites and carbonate rocks, which contain assemblages of magnetite-feldspar-amphibole-haematite-carbonate, developed for 1-2 km away from known Cu deposits. Magnetite is disseminated throughout footwall quartzites and also forms veinlets cross-cutting and paralleling primary layering. Pink feldspar-amphibole forms small layer-parallel and cross-cutting veinlets, which can also contain epidote and magnetite (Fig. 7e). Regional fabrics and shear zones are commonly overprinted by radial growths of dark green hornblende (Fig. 7f).

Other Significant Cu Deposits in the KCB

Akwali

Akwali, located about 15 km south of Khetri (Fig. 5), is a small Cu deposit (1.23 million t @ 1.7% Cu, 0.5-0.6 ppm Au, 6-8 ppm Ag) hosted by graphitic schist. Mineralisation is located along a sub-vertical NE-striking fault, extends for a strike length of about 5 km and comprises massive zones of chalcopyrite-pyrrhotite-pyrite and carbonate-chalcopyrite-pyrrhotite veins in silicified, carbonate-altered graphite schist. Iron oxides are not present in the ore-zone or associated alteration zones at Akwali. Several other fault-controlled graphitic-schist hosted Cu prospects occur around Akwali.

Kho Dariba

Kho Dariba, located 120 km SE of Khetri (Fig. 2), is hosted by a sequence of massive quartzite, carbonaceous phyllite with cordierite and andalusite, and biotite-muscovite schist. The deposit is sited along the axial-plane of a moderately S-plunging antiform, and consists of a number of small impersistent subvertical shoots (GSI, 1994). These shoots contain veins and stockworks of quartz-pyrrhotite-chalcopyrite and amphibole-biotite-calcite-chalcopyrite-pyrrhotite. Proximal alteration assemblages enveloping vein-sets and stockworks extend for 5-10 m into host rocks and comprise biotite-sericite-carbonate-pyrrhotite-chalcopyrite assemblages. These grade into outer alteration assemblages of amphibole-carbonate-pyrrhotite, with variable biotite and magnetite.

Other Deposits in the KCB

In addition to Cu mineralisation, the KCB hosts deposits of fluorite, Fe-ore, baryte and uranium. The nature of these is summarised below.

Fluorite deposits at Chowkri-Chhapoli are hosted by granitoid, biotite schist and feldspathic quartzite and are associated with calcite-quartz-apatite-hornblende-chalcopyrite veins, with albite-haematite-magnetite wallrock alteration within host rocks (Ranawat, 1979).

Baryte and Cu-baryte deposits occur around Alwar (Fig. 2), in the eastern part of the KCB, where they form subvertical, NE- and NW-striking shear-zone hosted reefs in quartzites and carbonates (Sen Gupta and Bose, 1943; Jain, 1987). Mineralised veins are 1-2 m thick, contain coarse-grained baryte-chalcopyrite-magnetite-haematite, and are enveloped by narrow (<1 m) sericite-haematite-magnetite proximal alteration haloes and wider (5-20 m) distal alteration haloes of albite-haematite-magnetite.

Iron ore deposits, normally comprising sub-equal specular haematite and magnetite, with lesser carbonate, quartz, and apatite, occur throughout the KCB, and generally form massive veins and pods. Iron ore deposits at Morija-Banol, near Jaipur (Fig. 2) are haematite-dominant, with subordinate magnetite and minor apatite, are hosted by coarse-grained quartzites and conglomerates, and form anastomosing veins, reefs and breccia systems with albite-haematite alteration in host rocks (Israili and Absar, 1978). Patwardhan et al. (1987) ascribed a sedimentary origin for magnetite±apatite deposits at Antri-Biharipur, Dhanota and Sior, near Narnaul (Fig. 2), which are hosted by quartzites and carbonates, with abundant pink feldspar-carbonate-epidote-actinolite alteration.

Uranium–Th deposits have been described from several localities in the KCB, but they appear to be concentrated in a NE-SW striking zone lying to the SE of Khetri (Fig. 2). Uraninite-pyrite-pyrrhotite-chalcopyrite-molybdenite-carbonate-fluorite veins at Khandela, SW of Khetri, are hosted by brick-red granitoids, albite-haematite-magnetite breccias and amphibole-albite-haematite-calcite-magnetite rock (Narayan Das et al., 1980; Ray, 1987). Ray (1987) also documented

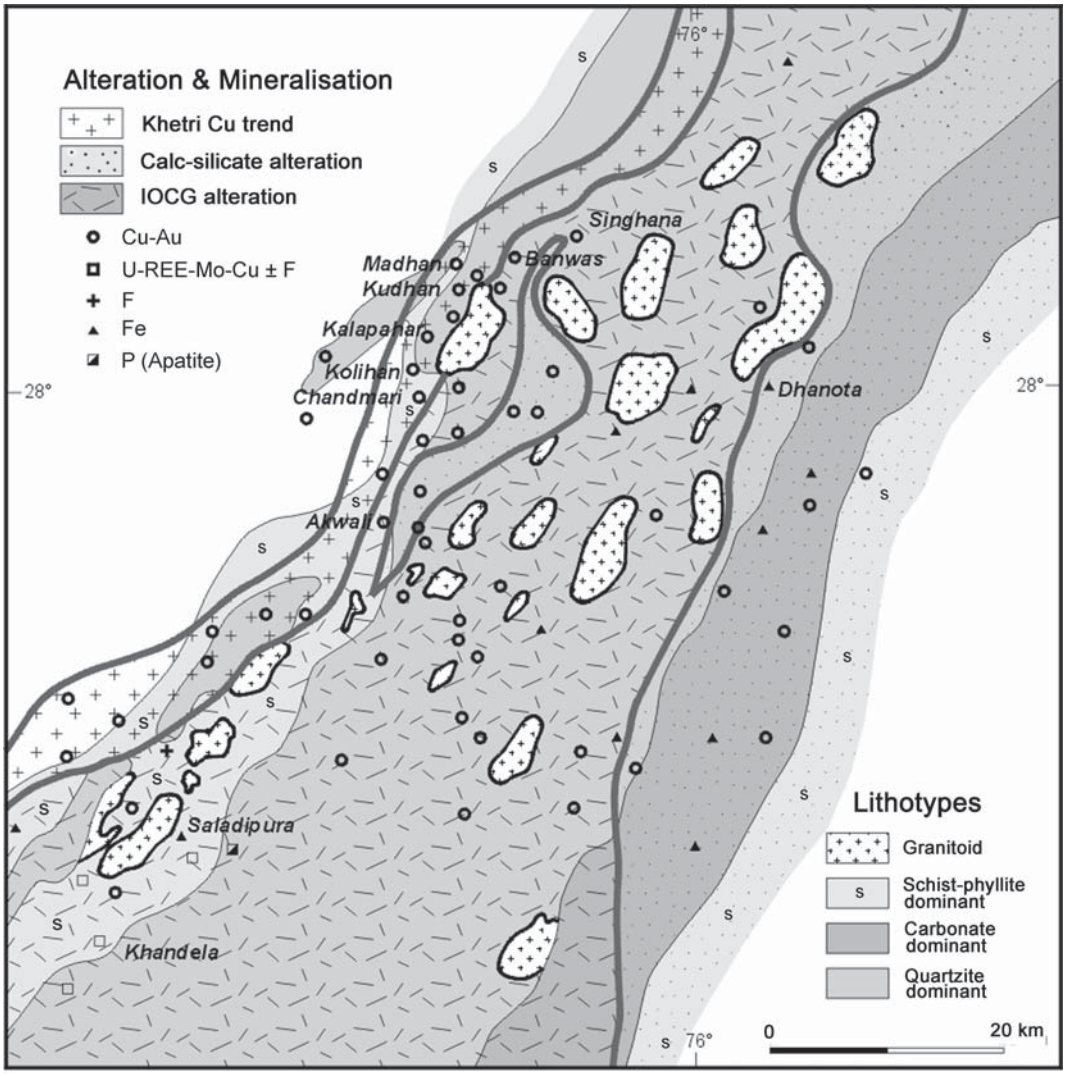

Figure 5: Geology of the Khetri area showing principal rock types, location of mineral deposits, and the distribution of regional alteration types.

chlorite-albite breccias and assemblages of scapolite-tremolite-titanite-apatite-chlorite-calcite associated with U mineralisation at Khandela.

Geochemistry of KCB Cu Ores

Whole rock geochemical analyses of ore samples from Cu deposits at Khetri, Kho Dariba, Gol, Pratapgarh and Nagel, and Cu-baryte deposits at Jamrauli and Makroda (located in Fig. 2) have been determined in order to provide quantitative analytical data on the elemental associations of mineralisation in the KCB. Samples from Khetri include representative composite mill-feed samples from Banwas, Madhan-Kudhan, Chandmari and Kolihan (Table 2). Samples from other deposits are representative grab samples of typical ore types.

Composite feed samples from Khetri show a Cu-Au-Co-S metal association, with elevated Mo and W (Table 2). Lead (<10) and Zn (40-60 ppm) are not enriched, and most metals are at low levels. Of the major elements, only Fe is elevated (14-16%), consistent with the Fe-sulphide rich nature of ore, whereas alkalis are low. Light rare earth elements are moderately elevated and U is low (<2 to 4 ppm). Analysed samples of typical ore from Kho Dariba are enriched in Cu (830-76900 ppm) and Au (6-135 ppb), and variably enriched in Ag (<1 to 12.5 ppm), Ba (14-367 ppm), Bi (0.5-341 ppm), Mo (1.2-204 ppm), Pd (<1 ppb to 35 ppb), U (2.25-63.9 ppm) and LREE (La = 7.5-38.3 ppm). Similar to Khetri, Pb and Zn are present at low levels. Copper deposits at Gol, Nagel and Pratapgarh are also characterised by elevated Cu and Au, with Gol distinguished by elevated As (1620 ppm). Samples of vein material from Cu-baryte deposits at Jamrauli and Makroda are enriched in Ba (3.59-25.3%), Ag (0.5-566 ppm), Au (2-1740 ppb), Cu (65-17700 ppm) and Mo (0.4-39.4 ppm), with variable enrichments in LREE (La = 2.05-23.7 ppm), Bi (1.3-43.5 ppm) and Te (<0.1-18.8 ppm). A Cu-Au signature therefore characterises all copper deposits across the KCB, with associated enrichment in Ag, Ba, Bi, Mo and LREE.

Fluid Properties of Khetri Ores

There are few published data to constrain the P-T conditions and composition of the fluids that deposited, mineralisation at Khetri. Jaireth (1984) analysed fluid inclusions in quartz, pyrite and calcite from three phases of mineralisation identified at Madhan Kudhan and Kolihan. Early barren quartz was deposited from low-salinity, low-density fluids at 540-560°C, whereas ore-related quartz and sulphides were deposited from dense highly-saline (50 wt% NaCl equivalent) fluids in the temperature range 280-480°C. Late unmineralised calcite veins were deposited from low density, moderately saline fluids (23 wt% NaCl equivalent) at 240-260°C. Sahu et al. (1977) estimated that vein quartz from mineralised veins at Kolihan was deposited at >350°C from highly saline fluids (33 wt% NaCl and 17 wt% KCl equivalent).

Sulfur isotope compositions of chalcopyrite and pyrrhotite from Madhan Kudhan ($\delta^{34}S$ = +5.5 to +9.2 per mil) and Kolihan ($\delta^{34}S$ = +5.3 to +8.1 per mil) are broadly similar (Jaireth, 1986), and overlap with the S isotope composition of a number of potential fluid sources, including granitoids, mafic rocks and evaporites (Rollinson, 1993).

Nature of Regional Alteration in the KCB

The KCB contains widespread regional alteration. Two main types can be classified on the basis of mineralogy and texture: (1) calc silicate alteration and (2) albite-haematite alteration. The mineralogy, texture, and temporal and spatial relationships of these alteration types to the widespread Cu-Au-Ag-Ba-Bi-Mo-LREE and Fe ore mineralisation in the KCB are discussed in the following sections.

Calc Silicate Alteration: Mineralogy and Textures

Calc-silicate alteration comprises assemblages of amphibole, clinopyroxene (diopside), scapolite, albite and calcite, with variable epidote, apatite, titanite, specular haematite and magnetite (Fig 7g). Assemblages are generally very coarse grained and are developed in undeformed pods and veins, which both parallel and cross-cut metamorphic and primary layering. Calc silicate minerals also form massive coarse-grained bodies which have entirely replaced primary mineralogy and texture. Typically, alteration consists of simple mono- or bi-minerallic assemblages of clinopyroxene-amphibole, which are cross-cut by veinlets of scapolite, albite or calcite. Titanite, magnetite and apatite are normally present as accessory phases, finely disseminated through altered rocks.

Calc silicate alteration is developed in all rock types in the KCB, but is preferentially developed in carbonate rocks where assemblages of coarse bladed pyroxene-amphibole-calcite, with lesser apatite and scapolite are developed. Altered granitoids and quartzites contain veinlets of calcite-pyroxene-apatite-amphibole-magnetite. Elsewhere, assemblages of calc silicate minerals form complex hydrothermal breccias, comprising clasts of amphibole-clinopyroxene altered metamorphosed sedimentary rock, monominerallic amphibole and amphibole ± albite ± haematite, in a matrix of very coarse-grained euhedral calcite (Fig. 7h). These breccias commonly host chalcopyrite-pyrite mineralisation and can contain abundant magnetite.

Albite-haematite Alteration: Mineralogy and Textures

In contrast to calc silicate alteration, albite-haematite alteration is not restricted to particular lithologies, and is developed to varying degrees in all rock types in the KCB. Albite-haematite alteration typically comprises assemblages of pink to red albite-amphibole-magnetite-haematite-calcite, with locally abundant K-feldspar, biotite, scapolite, chlorite, epidote and titanite, and variable but

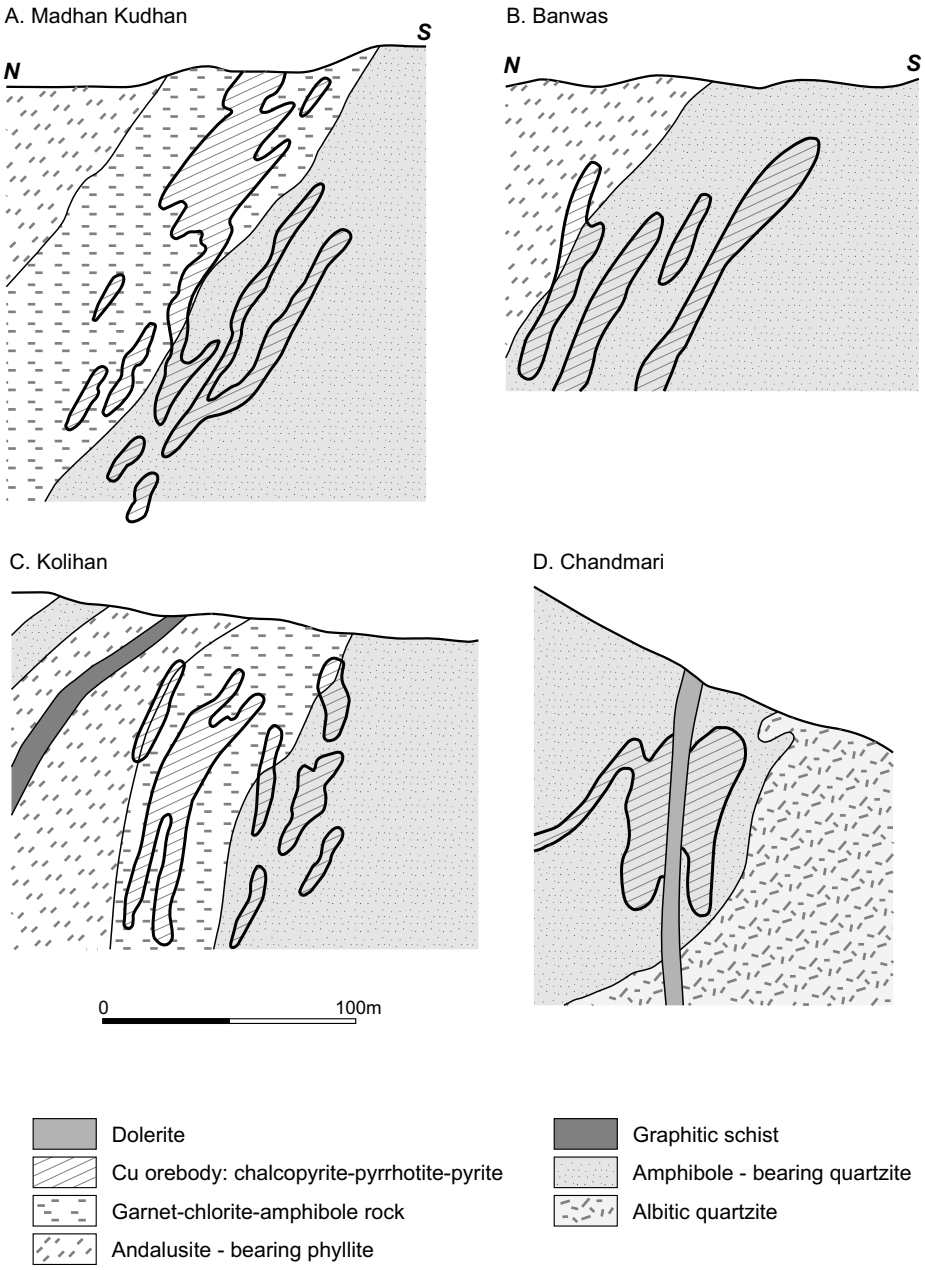

Figure 6: Schematic cross sections through Cu-Au-Ag orebodies at Khetri, Rajasthan (based on unpublished Hindusthan Copper Ltd data).

Figure 7 (facing page): Mineralisation and alteration styles at Khetri and calc-silicate alteration

- **A** Massive chalcopyrite-pyrrhotite ore with amphibole-biotite alteration, Madhan Kudhan.
- **B** Massive to weakly foliated garnet-chlorite-amphibole rock, with coarse chalcopyrite-pyrrhotite, Madhan Kudhan.
- **C** Banded amphibole-plagioclase rock, with weakly disseminated haematite-magnetite, cross cut by quartz-chalcopyrite-pyrrhotite veins, Chandmari.
- **D** Banded-foliated amphibole-albite rock cross-cut by veinlets and stockworks of chalcopyrite-pyrrhotite-magnetite-biotite, Chandmari.
- **E** Steeply dipping feldspathic quartzites overprinted by amphibole-pink albite alteration, Chandmari haul road.
- **F** Strongly foliated coarse-grained conglomeratic rocks overprinted by randomly oriented coarse hornblende, south of Khetri deposits.
- **G** Massive coarse-grained clinopyroxene-amphibole alteration, with lesser feldspar and scapolite and and minor titanite.
- **H** Breccia comprising metre-scale clasts of amphibole-pyroxene altered meta-sedimentary rock in a matrix of very coarse-grained calcite.

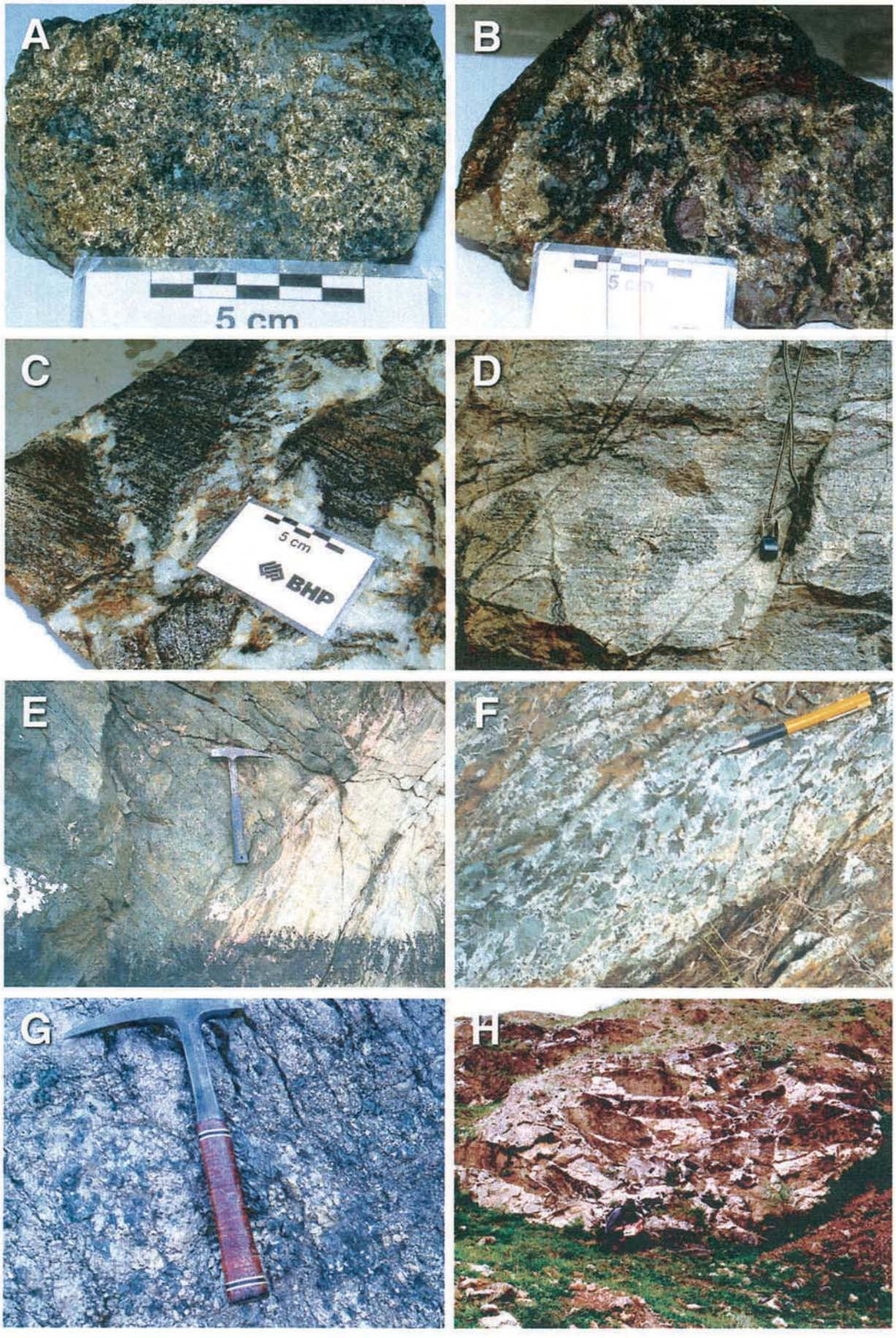
A
5 cm
B
5 cm
C
5 cm
BHP
D
E
F
G
H

Reverse of colour plate, intentionally blank

generally minor amounts of fluorite, pyrite, chalcopyrite and molybdenite (Fig. 8a to 8h). Quartz is generally rare or absent from this alteration, and is typically restricted to veins. In weakly- to moderately-developed alteration zones, rocks are pervasively dusted with haematite, quartzites are pink to red and metamorphosed intermediate volcanic rocks contain pink calcic plagioclase partly or completely altered to albite. Primary lithological textures are preserved. With greater degrees of alteration, metamorphic mineralogy and textures are entirely replaced by banded albite-haematite-magnetite-amphibole rock. At the outcrop scale, multiple phases of alteration can be identified: early pink, layer-parallel albite-disseminated haematite is cross-cut by multiple phases of progressively darker red albite-haematite-amphibole alteration (Fig. 8a and 8b).

Copper mineralisation is commonly developed within regional albite-haematite alteration, where it forms pipe-like bodies comprising multiple vein-sets and stockworks, which generally cross-cut banded albite-haematite-magnetite-calcite-amphibole rocks (Fig. 8e). Vein-fill comprises calcite-quartz-amphibole-chalcopyrite-pyrite. Other vein styles commonly developed in albite-haematite alteration include magnetite-haematite-quartz veins, enveloped by albite-haematite-amphibole-magnetite alteration (Fig. 8f), and calcite-apatite-amphibole veins enveloped by pink albite alteration (Fig. 8g). Complex breccia systems are commonly developed and generally comprise angular and rounded fragments of magnetite-amphibole-albite-haematite in a matrix of albite-haematite-calcite-magnetite-amphibole, with minor chalcopyrite-pyrite, and malachite in weathered samples. Establishing paragenetic relationships of discrete phases within regional albite-haematite alteration zones is complicated by multiple overprinting relationships, with several phases of alteration and mineralisation identifiable at outcrop-scale.

Distribution and Zonation of Alteration Types

Regional calc silicate and albite-haematite alteration is developed throughout the KCB, extending over an area of around 100 km wide by 100 km NE strike-length. Alteration probably continues further to the north and south under thick sand dunes and colluvium. In general, the alteration types occur in regional-scale domains. To the east of Khetri, albite-haematite alteration forms a 15-20 km wide central corridor, flanked by >15 km domains where calc silicate alteration is dominant (Fig. 5). These corridors of alteration show a spatial relationship with regional-scale NE-striking faults, which potentially represent re-activated early rift faults (Singh, 1988). The most intense alteration, and associated mineralisation, is developed around intersections of NE- or NNE- and NW-striking faults. At the regional-scale, the most intense albite-haematite alteration appears to be developed where there is a concentration of post-tectonic granitoids to the east of mineralisation at Khetri.

Element-associations of mineralisation are broadly zoned across the KCB, ranging from Cu only at Akwali, to Cu-Au at Khetri and Kho Dariba, to Cu-Au-Fe-Mo-REE-U in albite-haematite regional alteration to the east of Khetri, and Cu-Au-Ba-Ag around Alwar. This chemical variation is reflected in the sulphide-oxide-sulfate mineralogy associated with Cu ores across the KCB, with four dominant types recognised: (1) chalcopyrite-pyrite-pyrrhotite ores hosted by graphitic schists at Akwali in the south west of the KCB, (2) chalcopyrite-pyrite-pyrrhotite-magnetite-haematite ores at Khetri and Kho Dariba, in the east, (3) magnetite-haematite-chalcopyrite-pyrite ores hosted by albite-haematite alteration in the central part of the KCB, and (4) haematite-chalcopyrite-baryte ores in the eastern part of the Belt.

Timing of Mineralisation and Wallrock Alteration

Within the KCB, calc silicate and albite-haematite alteration assemblages, and associated mineralised veins and structures, are generally undeformed and overprint peak-metamorphic assemblages and fabrics. At Khetri, mineralised veins and associated alteration haloes cross-cut regional NE-striking fabrics (eg., Fig. 7c to 7f). Where calc silicate and albite-haematite alteration occur together, assemblages of albite-haematite-amphibole-magnetite appear to overprint calc silicate minerals (Fig. 8h). The silicate mineralogy of wallrock alteration at Khetri (amphibole, biotite-garnet, chlorite) and the mineralogy of both calc silicate and albite-haematite alteration suggest that regional alteration and Cu mineralisation at Khetri formed at relatively high temperatures (low-amphibolite facies).

There are currently no available precise age determinations of Cu mineralisation in the KCB. A mean fission track age of 897±125 Ma has been determined for garnet from ore assemblages at Madhan-Kudhan (Singh et al., 1988). The timing of regional alteration in the KCB is constrained to 847±8 Ma by the SHRIMP U-Pb age of titanite in the assemblage albite-haematite-amphibole-calcite-titanite (Fig. 4b, data are presented in Appendix 1). This suggests that the timing of regional alteration potentially overlaps with both Cu mineralisation and post-tectonic granitoid emplacement.

Relationship Between Cu-Au Mineralisation and Regional Alteration in the KCB

In order to establish whether the KCB is an IOCG terrane, it is necessary to determine the relationship between the widespread Cu mineralisation and regional calc silicate and albite-haematite alteration. The following evidence suggests a genetic and temporal relationship between the two:

1) Both regional alteration and mineralisation are controlled by late brittle and brittle-ductile NE- and NW-striking faults.
2) Textural relationships indicate that Cu mineralisation and regional alteration post-date the main phases of metamorphism and deformation.
3) Similar silicate minerals define ore-related wallrock-alteration assemblages at Khetri (ie., amphibole-

Table 2: Multi-element analyses of composite millhead samples from Khetri and grab samples from other Cu prospects in the KCB

Sample	KCC1	KCC2	KCC3	KCC4	KCC5	KCC6	KCC7	Kho Dariba	Jamrauli	Nagel	Makroda	Pratapgarh	Gol
Major elements (%)													
Si	27.9	19.8	27.1	2.99	2.37	29.2	30.5	na	na	na	na	na	na
Ti	0.28	0.19	0.28	0.03	0.03	0.28	0.28	0.11	0.03	0.03	0.25	0.41	0.59
Al	3.79	2.36	4.26	0.54	0.44	3.75	4.47	3.26	0.84	0.71	4.52	7.12	2.83
Fe	15.9	16.6	14.2	38	42	15	12.4	5.64	0.75	2.13	7.17	2.75	1.19
Mn (p	1830	595	1700	259	301	1940	1720	932	33	78	464	170	119
Mg	2.31	7.03	2.31	0.39	0.31	2.25	2.45	1.29	0.05	0.06	0.93	0.59	0.1
Ca	0.92	2.94	0.82	0.12	0.11	0.9	0.84	1.69	0.04	0.04	0.13	0.04	0.72
Na	0.61	0.36	0.7	0.1	0.1	0.57	0.71	0.07	0.04	0.03	0.1	0.09	2.25
K	0.74	1.81	0.9	0.16	0.11	0.71	0.94	2.03	0.25	0.12	5.01	3.88	0.09
P (ppr	420	440	440	80	80	440	420	na	na	na	na	na	na
S (ppr	38400	56900	34200	320000	335000	14000	12100	22300	56000	200	3120	200	340
Trace elements (ppm)													
Ba	97	82	115	22	20	128	125	145	253000	54	138000	434	21
Cs	1.7	3.2	1.9	0.3	0.3	1.7	2	na	na	na	na	na	na
Li	11.5	11.5	12.5	1.5	1	13	14	na	na	na	na	na	na
Rb	50.7	154	61.6	8.82	6.76	46.8	61.9	na	na	na	na	na	na
Sr	15.5	14.1	17.3	3.6	3.1	16.2	18.5	na	na	na	na	na	na
Tl	0.3	0.3	0.4	1.4	1.7	0.2	0.3	na	na	na	na	na	na
U	4.15	2.25	4.25	3.25	3.2	4.6	5.1	63.9	2.2	1.65	2.8	5.55	3.3
V	80	40	84	16	18	78	84	na	na	na	na	na	na
Metals and ore elements (ppm)													
Ag	1	1	1	13.5	12	bdl	bdl	5	566	8	2	bdl	bdl
As	9.5	12.5	16.5	60	121	3.5	4.5	1.5	58	30.5	bdl	36.5	1620
Au (p	273	2250	302	1930	2450	123	143	87	64	1510	215	4	195
Bi	2.2	0.4	4.2	13.6	24	1.4	1.9	14.5	39.5	3.3	1.3	0.2	0.4
Cd	bdl	bdl	bdl	1	1	bdl	bdl	2	bdl	bdl	bdl	bdl	bdl
Cr	85	100	115	20	20	200	110	na	na	na	na	na	na
Cu	13700	25400	11900	180000	141000	2280	1490	18400	17700	53400	6830	203	9890
Co	130	140	118	708	808	108	74	na	na	na	na	na	na
Mo	9	2.4	5.4	35.2	26.4	101	9	204	5.6	2	0.4	23.8	1.6
Ni	82	104	77	350	448	62	56	na	na	na	na	na	na
Pt (pp	bdl	5	5	5	bdl	bdl	bdl	10	bdl	bdl	bdl	bdl	bdl
Pd (p	5	10	10	25	20	bdl	5	bdl	bdl	5	bdl	bdl	bdl
Pb	6	3	10	24	41	13	8	3	12	bdl	3	10	3
Sb	bdl	0.2	0.2	0.6	1.2	0.2	bdl	2	0.4	0.4	0.2	3.6	0.4
Se	3	6	2	23	24	2	2	bdl	bdl	17	bdl	4	9
Sn	8	9	7	51	43	6	5	bdl	na	na	na	na	na
Te	0.2	0.4	0.2	1.6	1.4	bdl	bdl	bdl	bdl	bdl	bdl	bdl	0.4
W	8.5	4.5	11	3.5	4	10.5	11.5	1.5	1.5	1	3	2.5	3
Zn	61	43	65	396	328	92	54	91	5	17	17	15	12
Rare earth elements (ppm)													
La	37.6	33.6	38.3	13	15.3	39.4	36	10	3.05	13	23.7	5.75	3.65
Ce	71	55.3	73.8	24.9	29.1	75.7	67	20.5	6.85	27.3	51.9	16.1	10.5
Pr	7.76	6.14	8.24	2.8	3.28	8.5	7.4	na	na	na	na	na	na
Nd	32	26.2	33.1	11.5	13.1	33.5	32.3	na	na	na	na	na	na
Sm	7.2	8.6	7.4	2.7	3.2	8.15	7	na	na	na	na	na	na
Eu	2.26	1.68	2.18	0.78	0.92	2.56	2.12	0.36	bdl	1.06	bdl	0.3	0.62
Gd	7.4	11.6	7.4	2.6	3.2	8	7.4	na	na	na	na	na	na
Tb	1	1.82	0.98	0.34	0.38	1.18	0.96	na	na	na	na	na	na
Dy	5	10	5	1	2	6	5	3.85	0.35	2.2	1.35	2	15.1
Ho	1.02	1.78	0.82	0.22	0.26	1.06	0.82	na	na	na	na	na	na
Er	2.4	4	2.15	0.55	0.65	3.15	2.2	na	na	na	na	na	na
Tm	0.32	0.52	0.3	0.08	0.08	0.4	0.3	na	na	na	na	na	na
Yb	2.15	3.15	1.95	0.45	0.45	2.55	2.05	na	na	na	na	na	na
Lu	0.3	0.38	0.28	0.06	0.06	0.36	0.28	0.2	0.06	0.04	0.16	0.26	1.44

SAMPLE DESCRIPTIONS
KCC1. Khetri Mine, Banwas area 180 ML
KCC2. Rougher Feed. Composite sample from Khetri, Kolihan, Chandmari, May 1999
KCC3. Rougher Feed. Composite sample from Khetri, Kolihan, Chandmari, June 1999
KCC4. Final concentrate sample from Khetri, Kolihan, Chandmari, May 1999
KCC5. Final concentrate sample from Khetri, Kolihan, Chandmari, June 1999
KCC6. Final tail sample from Khetri, Kolihan, Chandmari, May 1999
KCC7. Final tail sample from Khetri, Kolihan, Chandmari, May 1999
Elements were analysed using a combination of fire-assay, ICP-MS and ICP-OES techniques. Bdl = below detection limit, na = not analyzed.

Figure 8 (facing page): IOCG alteration and vein styles

A Layered feldspathic-quartzite, with primary layering preserved, overprinted by pink albite-amphibole-calcite-magnetite alteration.

B Layered quartzite with intense layer-parallel amphibole alteration zone, cross-cut by veins and pods of pink (haematite-dusted) albite and amphibole

C Pink-red haematite-dusted feldspar-amphibole-calcite-magnetite-titanite alteration with angular clasts of albitized quartzite.

D Radial clusters of amphibole over-printing massive pink-red haematite-dusted albite-amphibole-magnetite-titanite rock.

E Calcite-chalcopyrite-pyrite-magnetite vein enveloped by red albite alteration in banded biotite-magnetite-pink albite rock.

F Quartz-magnetite-haematite veins enveloped by banded-foliated pink albite-magnetite-amphibole rock.

G Calcite-amphibole-apatite vein, enveloped by pink albite-amphibole alteration, cross-cutting layered feldspathic quartzite with pink albite-amphibole-magnetite alteration.

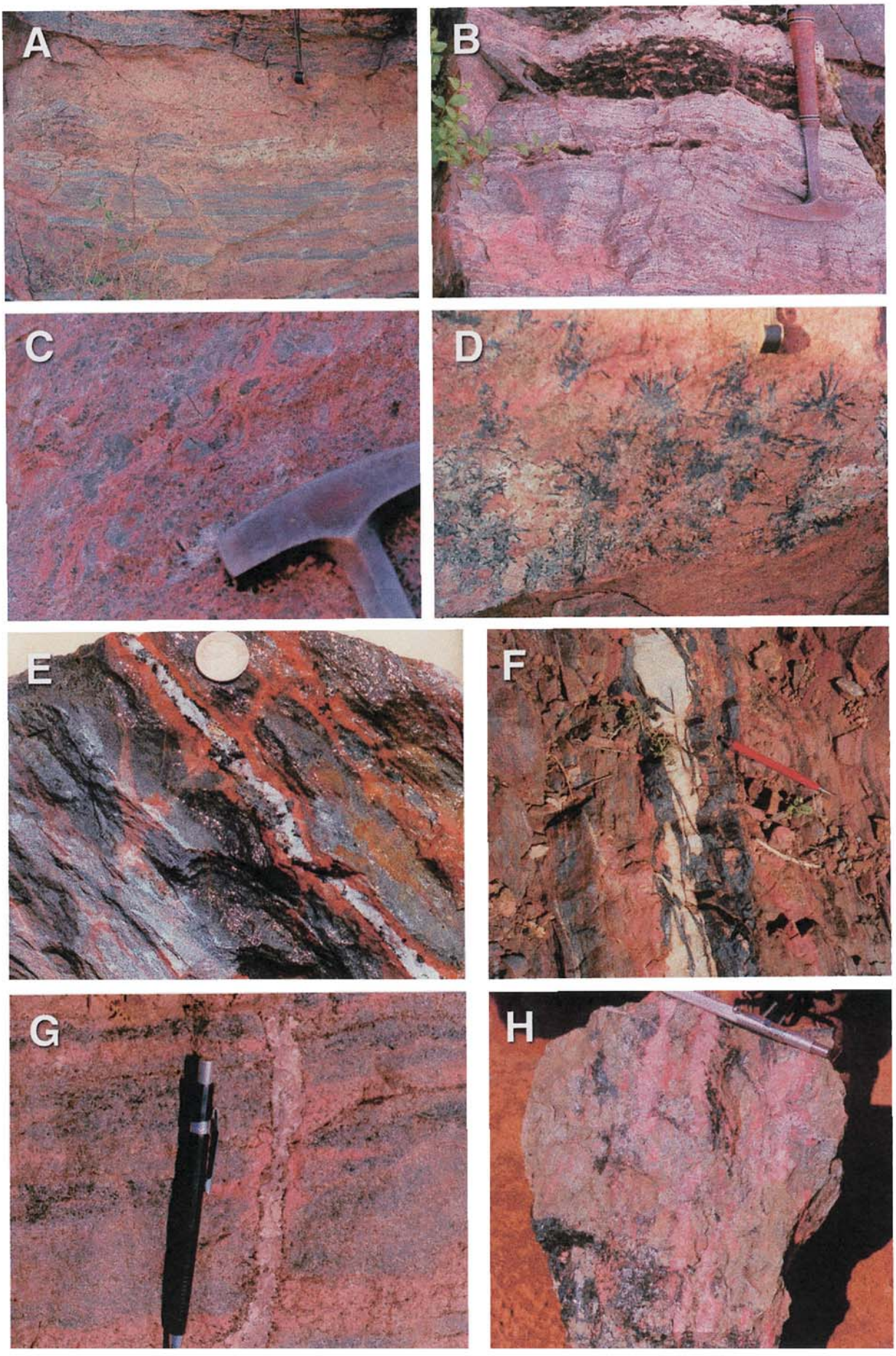
A
B
C
D
E
F
G
H

Reverse of colour plate, intentionally blank

albite-biotite-scapolite-magnetite) and regional alteration assemblages, suggesting that they formed from hydrothermal systems with a broadly similar composition at similar P-T conditions.

4) Camp-scale alteration assemblages associated with mineralisation at Khetri are characterised by similar mineralogy to regional-scale alteration (ie., amphibole-albite-haematite-magnetite-carbonate, Fig. 7e and f and Fig. 8).
5) Albite-haematite and calc silicate alteration host numerous Cu±Au±Ag±Ba±Co±Fe±U±REE deposits, with no known Cu deposits located outside the area of regional alteration.
6) Diverse styles of Cu mineralisation and associated alteration haloes across the KCB are characterised by similar geochemical enrichments and silicate-sulphide mineralogy.
7) Available age determinations suggest that mineralisation at Khetri and regional IOCG alteration formed broadly synchronously.

Comparison of KCB to Known Iron Oxide Copper-Gold Deposits

Several features of mineralisation and regional alteration in the KCB are similar to those in well-documented IOCG mineralised terranes worldwide (eg., Haynes, 2000; Hitzman, 2000), namely:

1) Mineralisation is sited within a regional-scale alteration system characterised by assemblages of calc silicate minerals (amphibole-clinopyroxene-scapolite-albite-calcite) and assemblages of albite-magnetite-haematite-amphibole-calcite.
2) Copper mineralisation is associated with variable enrichments in Au, Ag, Ba, Co, F, Fe, REE and U.
3) Regional alteration and Cu mineralisation post-date peak metamorphism and deformation.
4) Mineralisation is commonly hosted by, and regional alteration is spatially controlled by, late dominantly brittle faults.
5) Regional alteration and Cu deposits show a broad spatial and temporal relationship with post-tectonic A-type granitoids.
6) Available fluid inclusion data indicate that mineralisation was deposited from highly saline fluids at 280-480°C.

It is proposed therefore that mineralisation in the KCB can be classified as belonging to the Proterozoic iron oxide copper-gold deposit class. Within the KCB, there is a range of iron sulphide Cu-Au and iron oxide Cu-Au deposits and related ore types (cf., Haynes 2000; Hitzman 2000). Mineralisation types include (1) chalcopyrite-pyrrhotite-pyrite ores hosted by reduced graphitic schists (eg., Akwali), (2) chalcopyrite-pyrite-pyrrhotite±magnetite±haematite ores located at the transition between reduced and oxidised rocks (eg., Khetri), (3) magnetite-haematite-chalcopyrite-pyrite deposits hosted by oxidised rocks within regional albite-haematite alteration, (4) magnetite-haematite-apatite deposits (eg., Morija-Banol), and (5) baryte-chalcopyrite-haematite-pyrite ores (eg., Jamrauli, Makroda). Unifying features of mineralisation in the KCB are the structural controls, brittle-nature and late-timing of mineralisation, and the broad geochemical associations and alteration mineralogy of the different ore types.

Summary and Conclusions

The Khetri Copper Belt, and associated sub-parallel copper belts, host widespread Cu±Au±Ag±Co±Fe±Mo±REE±U mineralisation over a 150 km by 150 km area of NW India. These deposits are all:

1) structurally controlled by NE- and NW-striking late faults,
2) texturally late and overprint regional metamorphic and deformation fabrics,
3) enveloped by alteration assemblages containing a combination of the following minerals: albite, amphibole, Fe oxide (haematite or magnetite), carbonate, biotite, epidote, apatite, scapolite and titanite,
4) characterised by simple sulphide assemblages of chalcopyrite±pyrite±pyrrhotite,
5) enriched in Cu and Au, with variable enrichments in Ag, Co, Fe, Mo, REE, U, and
6) sited within regional-scale calc silicate and albite-haematite alteration systems.

These features, in combination with the spatial and temporal association of mineralisation with post-tectonic A-type granitoid emplacement and the gross tectonic setting of the host Delhi Supergroup, suggest that mineralisation in the KCB belongs to the iron oxide copper-gold deposit-class.

Recognition of the likely affinities of Cu mineralisation in the KCB, together with (1) the generally thick deposits of sand, alluvium and colluvium which limit out-crop in northern Rajasthan and Haryana and (2) the lack of IOCG-targeted regional exploration, suggest that the potential for making further discoveries is high.

Acknowledgements

Bob Melsom and Chris Woodman are thanked for drafting the figures, and Sue Buckley is gratefully acknowledged for her assistance in literature searches and data gathering. Tony D'Orazio and Ilam Panneerselvam are thanked for data processing, and Meena Sindhi and Richa Arora for all their assistance during fieldwork in India.

Hindusthan Copper is gratefully acknowledged for allowing access to the copper-gold mines at Khetri.

Marion Marshall and Neal McNaughton are thanked for assistance with the sample preparation and SHRIMP geochronology, respectively. Isotopic data were acquired on a Sensitive High Resolution Ion Microprobe Mass Spectrometer (SHRIMP II), which is operated by a consortium consisting of Curtin University of Technology, the Geological Survey of Western Australia and the

University of Western Australia, with the support of the Australian Research Council.

This paper benefited greatly from reviews by Douglas Haynes and John Ridley who are thanked for their input. This paper is published with the kind permission of BHP Billiton Ltd.

References

Banerjee, A.K., 1976 – Tectonics and ore location in northeastern Rajasthan, India, *Indian Minerals* 29, 1-24.

Basu, S.K., & Narsayya, B.L., 1982 – Carbonatite-alkali metasomatic rock association in the eastern part of Khetri Copper Belt, northeastern Rajasthan, *Indian Minerals* 36, 29-31.

Basu, S.K., & Narsayya, B.L., 1983 – A probable zone of carbonatite and fenitic rock association in the eastern part of the Khetri copper belt, northeastern Rajasthan, *Records of the Geological Survey of India* 113, 7-15.

Basu, S.K., 1986 – Petrology and geochemistry of the Singhana-Muradpur sulphide deposit: A Precambrian syngenetic copper deposit in the Khetri Copper Belt, Rajasthan, India, *Indian Minerals* 40, 1-16.

Blake, D.H., Etheridge, M.A., Page, R.W., Stewart, A.J., Williams, P.R. & Wyborn, L.A.I., 1990 – Mount Isa inlier – regional geology and mineralisation; *in* Hughes, F.E. (ed.), Geology of the Mineral Deposits of Australia and Papua New Guinea, *The Australian Institute of Mining and Metallurgy Monograph* 14, 915-925.

Choudary, A.K., Gopalan, K., & Shastry, C.A., 1984 – Present status of the geochronology of the Precambrian rocks of Rajasthan, *Tectonophysics* 105, 131-140.

Compston, W., Williams, I.S., & Meyer, C., 1984 - U-Pb geochronology of zircons from lunar breccia 73217 using sensitive high mass-resolution ion microprobe, *Journal of Geophysical Research* 89, Suppl. B, 525-534.

Crawford, A.R., 1970 – The Precambrian geochronology of Rajasthan and Bundelkhand, northern Indian, *Canadian Journal of Earth Sciences* 7, 91-110.

Cumming, G.L., & Richards, J.R., 1975. Ore lead isotope ratios in a continuously changing earth, *Earth and Planetary Science Letters* 28, 155-171.

Das Gupta, S.P., 1968 – The structural history of the Khetri copper belt, Jhunjhunu and Sikar districts, Rajasthan, Geological Survey of India Memoir 98, 170 pp.

Das Gupta, S.P., 1974 – Geological setting and origin of sulphide deposits in the Khetri copper belt Rajasthan, Bulletin Geological, Mining and Metallurgical Society of India 47, 221-238.

Dasgupta, S., 1978 – Sedimentary structures in the Precambrian Delhi Supergroup rocks and their significance, Indian Journal of Earth Sciences 5, 177-182.

Deb, M. & Sarkar, S.C., 1990 – Proterozoic tectonic evolution and metallogenesis in the Aravalli-Delhi orogenic complex, northwestern India, *Precambrian Research* 46, 115-137.

Deb, M., Thorpe, R.I., Krstic, D., Corfu, F. & Davis, D.W., 2001 – Zircon U-Pb and galena Pb isotope evidence for an approximate 1.0 Ga terrane constituting the western margin of the Aravalli-Delhi oreogenic belt, northwestern India, *Precambrian Research* 108, 195-213.

Gangopadhyay, P.K., 1974 – Some observations on the nature and origin of 'hornstone breccia' occurring within the Delhi Group in northeastern Rajasthan, *Proceedings 61st Indian Science Congress*, 163

Gangopadhyay, P.K., & Sen, R., 1967 – On the occurrence of andalusite near Bairwas, Alwar District, Rajasthan, *Proceedings 54th Indian Science Congress*, p. 220.

Geological Survey of India, 1994 - Detailed information on copper-lead-zinc ores in Rajasthan-Gujarat, India, *Geological Survey of India Publication.*

Gopalan, K., Trivedi, J.R., Balasubrahmanyan, M.N., Ray, S.K., & Sastry, C.A., 1979 – Rb-Sr geochronology of the Khetri Copper Belt, Rajasthan, *Journal Geological Society of India* 20, 450-456.

Haynes, D.W., 2000 – Iron oxide copper (-gold) deposits: their position in the ore deposit spectrum and modes of origin; *in* Porter, T.M., (ed), Hydrothermal Iron Oxide Copper-Gold & Related Deposits: A Global Perspective, *Australian Mineral Foundation, Adelaide*, pp 71-90

Heron, A.M., 1917 – Geology of Northeastern Rajputana and adjacent district, *Memoir Geological Survey of India* 45, 1-29.

Heron, A.M., 1922 – The geology of Western Jaipur, *Records of the Geological Survey of India* 54, 345-397.

Heron, A.M., 1953 – The geology of central Rajputana, *Memoir Geological Survey of India* 79, 1-339.

Hitzman, M.W., Oreskes, N., & Einaudi, M.T., 1992 – Geological characteristics and tectonic setting of Proterozoic iron oxide (Cu-U-Au-LREE) deposits, *Precambrian Research* 58, 241-287.

Hitzman, M.W., 2000 – Iron oxide-Cu-Au deposits: What, where, when, and why; *in* Porter, T.M., (ed), Hydrothermal Iron Oxide Copper-Gold & Related Deposits: A Global Perspective, *Australian Mineral Foundation, Adelaide*, pp 9-25.

Israili, S.H. & Absar, A., 1978 – Geology and structure of the Morija-Banol iron ore deposits, Jaipur district, Rajasthan, *Geoviews* 4, 17-34.

Jain, V.K., 1987 – Mining and geology of barytes deposit of district Alwar, Rajasthan, *Journal of Mines, Metals and Fuels* 35, 328-330.

Jaireth, S., 1984 – Ore paragenesis and fluid-inclusion thermometry of copper sulphide ores from Madhan-Kudhan and Kolihan deposits, *Special Publication Geological Survey of India* 12, 551-568.

Jaireth, S., 1986 – Igneous source of sulfur of sulphides from Madhan-Kudhan and Kolihan deposits, Khetri Copper Belt, Rajasthan, *Journal of the Geological Society of India* 27, 359-368.

Lal, R.K. & Shukla, R.S., 1975 – Low-pressure regional metamorphism in the northern portion of the Khetri Copper Belt of Rajasthan, India, *Neues Jahrbuch Mineralogy* 124, 294-325.

Nakamura, N., 1974 – Determination of REE, Ba, Mg, Na and K in carbonaceous and ordinary chondrites, *Geochimica et Cosmochimica Acta* 38, 757-775.

Narayan Das, G.R., Sharma, D.K., Singh, G 7 Singh, R., 1980 – Uranium mineralization in Sikar district, Rajasthan, *Journal of the Geological Society of India* 21, 432-439.

Neumayr, P., Ridley, J.R., McNaughton, N.J., Kinny, P.D., Barley, M.E., & Groves, D.I., 1998 - Timing of gold mineralization in the Mt. York district, Pilgangoora greenstone belt, and implications for the tectonic and metamorphic evolution of an area linking the western and eastern Pilbara Craton, *Precambrian Research* 88, 249-265.

Patwardhan, A.M., Patil, D.N. & Sukhtankar, R.K., 1987 – On magnetite quartzites occurring around Narnaul, Haryana, India; *in* Uitterdijk Appel, P.W., & G.L. LaBerge, G.L., (eds), Precambrian Iron Formations *Theophrastus Publications, Athens*, 513-537.

Pearce, J.A., 1983 – Role of the sub-continental lithosphere in magma genesis at active continental margins, *in* Hawkesworth, C.J. & Norry, M.J. (eds), Continental Basalts and Mantle Xenoliths. *Shiva*, 230-249.

Ranawat, P.S., 1979 – Nature of fluorspar mineralization at Chokri-Chhapoli, Sikar-Jhunjhunu districts, Rajasthan, *Journal Geological Society of India* 20, 24-30.

Ray, S.K., 1987 – Albitite occurrences and associated ore minerals in the Khetri Copper Belt, northeastern Rajasthan, *Records of the Geological Survey of India* 113, 41-49.

Ray, S.K., 1990 – The Albitite Line of northern Rajasthan – a fossil intracontinental rift zone, *Journal of the Geological Society of India* 36, 413-423.

Ray, S.K. & Ghosh, S.P., 1989 – The albitite dykes of Dudu sector in Jaipur district, Rajasthan, and their tectonic significance, *Indian Journal of Geology* 61, 129-132.

Rollinson, H.R., 1993 – Using geochemical data: evaluation, presentation, interpretation, *Longman Scientific & Technical, Harlow, Essex*, 352 p.

Roy Chowdhury, M.K. & Das Gupta, S.P., 1965 - Ore localization in the Khetri Copper Belt, Rajasthan, India, *Economic Geology* 60, 69-88.

Sahu, K.C., Panchapakesan, V. & Patil, R.R., 1977 – Fluid inclusion studies on samples from Kolihan Mines of Khetri Copper Belt, *Journal Geological Society of India* 18, 671-674.

Sarkar, S.C., Mukherjee, A.D., Bannerjee, H. & Sarkar, S., 1974 – A note on the pyrite-pyrrhotite mineralization at Saladipura, Sikar district, Rajasthan, *Indian Journal Earth Sciences* 1, 126-128.

Sarkar, S.C., & Dasgupta, S., 1980 – Geologic setting, genesis and transformation of sulphide deposits in the northern part of Khetri Copper Belt, Rajasthan, India – an outline, *Mineralium Deposita* 15, 117-137.

Sen Gupta, K.K. & Bose, A., 1943 – On the copper-barytes ore of Parisal in Alwar State (Rajputana) with a suggestive method of their separation, *Quarterly Journal Geological Mining and Metallurgical Society of India* 15, 151-152.

Singh, S.P., 1988 - Sedimentation patterns of the Proterozoic Delhi Supergroup, northeastern Rajasthan, India, and their tectonic implications, *Sedimentary Geology* 58, 79-94.

Singh, S., Singh, L., Singh, J., & Virk, H.S., 1988 – Fission track dating of some copper ore formations in India; in Khan-Hameed, A., Qureshi-Imtinan, E. & Ahmad-Ishfaq (eds), Solid State Nuclear Track detectors. Nuclear Tracks and Radiation Measurements, *Pergamon, Oxford*, 715-718.

Smith, J.B., Barley, M.E., Groves, D.I., Krapez, B., McNaughton, N.J., Bickle, M.J., &Chapman, H.J., 1998 - The Scholl shear zone, West Pilbara: evidence for a terrane boundary structure from integrated tectonic analyses, SHRIMP U-Pb dating and isotopic and geochemical data of granitoids, *Precambrian Research* 88, 143-171.

Whalen, J.B., Currie, K.L. & Chappell, B.W., 1987 – A-type granites: geochemical characteristics, discrimination and petrogenesis, *Contributions to Mineralogy and Petrology* 95, 407-419.

Appendix 1: SHRIMP Dating

Methods

SHRIMP methods follow Compston et al. (1984) and Smith et al. (1998) for zircons, and Neumayr et al. (1998) for titanite. The procedure involves focussing of an O_2^- ion beam to a 25-30 micron spot on sectioned and polished mineral grains, and measuring secondary ions to obtain isotopic ratios. Analyses were referenced to the CZ3 zircon and Khan titanite standards, analysed concurrently with the samples. The common Pb correction utilized the measured ^{204}Pb (Compston et al., 1984). Data in tables have errors of ±1 sigma, whereas uncertainties in pooled ages are quoted at the 95% confidence level.

Table A1: SHRIMP II isotopic data for zircons from the Gothra Granite.

CZ3 standard: n = 12, Calibration error = 0.89% (1 standard deviation).

Grain	U (ppm)	Th (ppm)_	Th/U	f206 (%)	207*/206*	208*/206*	206*/238	207*/235	208*/232	% conc.	207*/206* Age
1-1	285	147	0.52	0	0.1033±6	0.1504±10	0.3036±28	4.323±49	0.0884±10	102	1684±10
2-1	729	307	0.42	0.014	0.0988±4	0.1319±7	0.2774±24	3.781±37	0.0868±9	99	1602±7
3-1	1263	678	0.54	0.155	0.1033±3	0.1654±7	0.2824±24	4.024±37	0.0871±8	95	1685±6
4-1	282	93	0.33	0.017	0.1047±6	0.0965±11	0.298±28	4.302±50	0.0875±13	98	1709±11
5-1	320	102	0.32	0.096	0.1017±6	0.0934±10	0.2916±27	4.09±47	0.0853±13	100	1656±11
6-1	221	42	0.19	0.084	0.1132±7	0.0517±12	0.3391±33	5.292±65	0.0915±24	102	1851±12
7-1	205	69	0.34	0.075	0.1042±8	0.0951±16	0.3004±30	4.315±58	0.0845±17	100	1700±15
8-1	273	114	0.42	0.111	0.1028±6	0.1181±12	0.2993±28	4.244±51	0.085±13	101	1676±12
9-1	542	272	0.5	0.034	0.1035±4	0.1405±8	0.2986±26	4.262±43	0.0836±9	100	1688±7
10-1	343	127	0.37	0.048	0.1035±5	0.1088±9	0.2906±27	4.145±46	0.085±11	97	1687±9
11-1	432	177	0.41	0.079	0.1038±5	0.121±10	0.2941±26	4.21±45	0.087±11	98	1693±9
12-1	370	186	0.5	0.007	0.1041±5	0.1463±10	0.2971±27	4.266±46	0.0867±10	99	1699±9
13-1	253	108	0.43	0	0.1041±6	0.1206±10	0.2988±29	4.288±49	0.0845±11	99	1698±10
14-1	383	227	0.59	0.098	0.104±6	0.1797±13	0.2858±26	4.1±46	0.0866±10	95	1697±10
15-1	523	318	0.61	0.016	0.1035±4	0.1724±9	0.2983±26	4.259±43	0.0845±9	100	1688±8
16-1	245	102	0.42	0.001	0.105±7	0.122±13	0.295±28	4.272±53	0.0861±13	97	1715±12
17-1	241	100	0.42	0.105	0.1037±7	0.121±14	0.2983±29	4.267±54	0.0869±14	99	1692±13
18-1	178	58	0.33	0	0.1034±6	0.0934±10	0.3005±30	4.286±54	0.086±13	100	1687±12
19-1	662	343	0.52	0.032	0.1033±4	0.1485±8	0.2981±26	4.246±42	0.0856±9	100	1684±7
20-1	755	473	0.63	0.033	0.1037±3	0.1791±7	0.3014±26	4.309±41	0.0861±8	100	1691±6
21-1	286	130	0.45	0.036	0.1038±6	0.1291±12	0.2954±28	4.227±49	0.0839±11	99	1693±11
22-1	520	320	0.62	0.049	0.1036±4	0.1777±9	0.2974±26	4.248±43	0.0859±9	99	1690±8
23-1	278	109	0.39	0.003	0.1037±6	0.1111±12	0.3021±29	4.319±51	0.0858±13	101	1691±11
24-1	542	294	0.54	0.055	0.104±4	0.1563±9	0.2947±26	4.228±43	0.0849±9	98	1697±8

f206 (%) = % ^{206}Pb attributed to common ^{206}Pb.
Common Pb composition = coeval Cumming and Richards (1975) Model III Pb, corrected from ^{204}Pb.
Conc = concordance

Table A2: SHRIMP II isotopic data for titanite from Khetri

Grain	U (ppm)	Th (ppm)	Th/U	f206 %	207*/206*	208*/206*	206*/238	207*/235	208*/232	% Conc	207*/206* Age
10-2	49	147	3	0	0.0676±9	0.9061±92	0.1443±23	1.345±30	0.0436±9	101	856±29
2-2	94	362	3.88	0	0.0689±7	1.1858±85	0.1381±19	1.312±24	0.0423±7	93	896±22
7-5	48	157	3.3	0	0.0668±10	1.0094±101	0.1411±23	1.3±30	0.0432±9	102	832±30
8-2	38	109	2.89	0.152	0.066±20	0.8856±112	0.1442±25	1.312±49	0.0442±10	108	807±65
9-2	50	150	3.03	0.115	0.0665±16	0.919±100	0.1389±22	1.273±39	0.0422±9	102	821±50
1-2	38	108	2.8	0.572	0.0637±28	0.8538±130	0.1428±26	1.255±62	0.0435±11	117	733±93
14-2	92	353	3.82	0.265	0.0633±13	1.175±98	0.1391±19	1.214±32	0.0428±7	117	719±45
15-2	58	204	3.51	0.389	0.0638±21	1.0711±121	0.1412±22	1.242±48	0.0431±9	116	735±71
16-2	52	177	3.39	0	0.0673±11	1.0436±114	0.142±23	1.318±32	0.0438±9	101	848±32
17-1	38	109	2.87	0.153	0.0677±21	0.8554±125	0.1412±26	1.318±50	0.042±11	99	859±63
18-1	54	162	3	0.002	0.0685±16	0.9056±108	0.1392±23	1.316±39	0.0421±9	95	885±48
19-1	39	111	2.83	0.23	0.0685±25	0.8584±128	0.1427±26	1.348±58	0.0434±11	97	885±76
20-1	37	106	2.86	0.195	0.0654±32	0.8852±142	0.1426±27	1.286±70	0.0441±12	109	787±102
21-1	47	138	2.9	0.36	0.0669±25	0.8968±121	0.1386±24	1.278±55	0.0429±10	100	833±78
22-1	39	116	3	0.528	0.0645±34	0.9204±149	0.1401±26	1.247±73	0.043±11	111	759±112
23-1	40	111	2.76	0.728	0.0626±27	0.8316±126	0.1428±26	1.233±60	0.0431±11	124	696±93
24-1	43	122	2.87	0.132	0.0669±24	0.889±126	0.1388±25	1.281±54	0.043±11	100	836±74
25-1	42	119	2.83	0	0.0688±12	0.8577±110	0.1423±25	1.35±35	0.0432±10	96	892±35
26-1	40	113	2.86	0.046	0.0661±29	0.8621±130	0.1427±26	1.301±64	0.043±11	106	810±91
27-1	41	117	2.87	0	0.0679±12	0.9064±116	0.1377±24	1.289±34	0.0435±10	96	866±36
28-1	156	498	3.2	0.085	0.0669±10	0.9728±65	0.1412±17	1.301±26	0.0429±6	102	833±31
29-1	51	161	3.19	0.016	0.0672±18	0.9757±116	0.1435±24	1.33±44	0.0439±10	102	845±56
30-1	42	121	2.85	0.013	0.0683±23	0.8934±124	0.1377±24	1.297±51	0.0431±10	95	878±69
31-1	45	132	2.91	0.044	0.0669±20	0.8825±119	0.1391±24	1.282±47	0.0422±10	101	833±62
32-1	87	329	3.78	0.124	0.0658±17	1.173±105	0.1378±19	1.25±38	0.0427±8	104	801±53
33-1	171	522	3.06	0.006	0.0671±8	0.9191±60	0.1389±16	1.284±23	0.0418±6	100	840±26
34-1	40	111	2.8	0.177	0.0689±20	0.8958±124	0.1408±26	1.337±48	0.045±11	95	896±59
35-1	39	113	2.89	0.429	0.0657±36	0.8689±148	0.1384±26	1.254±75	0.0416±11	105	796±114
36-1	42	119	2.87	0.22	0.066±18	0.8816±122	0.1393±25	1.267±43	0.0428±11	104	807±56
37-1	53	156	2.93	0	0.0673±11	0.9127±111	0.1366±23	1.268±32	0.0426±10	97	847±34
38-1	47	142	3.01	0.404	0.0637±23	0.9032±120	0.1432±24	1.257±52	0.043±10	118	731±76
39-1	56	164	2.94	0	0.0695±11	0.8746±104	0.1414±24	1.354±33	0.042±9	93	912±33

Khan standard: Data collected during two sessions: n = 10 and 10, Calibration error = 1.14% and 1.00% (1 sigma).
f206 (%) = % ^{206}Pb attributed to common ^{206}Pb.
Common Pb composition = coeval Cumming and Richards (1975) Model III Pb, corrected from ^{204}Pb.
Conc = concordance.